New Journal of Physics
The open access journal at the forefront of physics

Deutsche Physikalische Gesellschaft DPG
IOP Institute of Physics

Published in partnership with: Deutsche Physikalische Gesellschaft and the Institute of Physics

OPEN ACCESS

RECEIVED
30 March 2020

REVISED
7 August 2020

ACCEPTED FOR PUBLICATION
13 August 2020

PUBLISHED
11 September 2020

PAPER

Precise measurements of polarizabilities of cesium *n*S Rydberg states in an ultra-cold atomic ensemble

Jingxu Bai[1], Suying Bai[1], Xiaoxuan Han[1], Yuechun Jiao[1,2], Jianming Zhao[1,2,3] and Suotang Jia[1,2]

[1] State Key Laboratory of Quantum Optics and Quantum Optics Devices, Institute of Laser Spectroscopy, Shanxi University, Taiyuan 030006, People's Republic of China
[2] Collaborative Innovation Center of Extreme Optics, Shanxi University, Taiyuan 030006, People's Republic of China
[3] Author to whom any correspondence should be addressed.

E-mail: zhaojm@sxu.edu.cn

Keywords: ultra-cold Rydberg atom, polarizability, Stark spectra

Abstract

We present precise measurements of polarizabilities of cesium $nS_{1/2}$ ($n = 65$–75) Rydberg states by Stark spectroscopies. In experiment, Rydberg atoms are excited via a two-photon scheme of a standard magneto-optical trap and detected by the field ionization technique. The Stark shift is measured by analysing the spectroscopy under an external electric field. The polarizability, α, is acquired by fitting the experimental data of Stark shifts with $\Delta W = -\frac{1}{2}\alpha E^2$. The theoretical model is applied to numerically simulate the Stark map and corresponding level shifts, related deviation between the experimental measurements and calculations are less than 2%. The scaling law of polarizabilities, $A \cdot (n^*)^7 + B \cdot (n^*)^6$ (n^* is effective principal quantum number), is attained, that shows a good agreement with the measurements.

1. Introduction

Atomic polarizability describes the response of an atomic system to an external field. Precise measurement of the atomic polarizability plays an important role both in proving the reliability of the theoretical model and experimental investigations and science applications like modern quantum technologies. Rydberg atom, with principal quantum number $n \gtrsim 10$, has big size ($\sim n^2$), long lifetime ($\sim n^3$), large polarizability ($\sim n^7$) and strong interaction ($\sim n^{11}$) [1] and so on. The characteristic of large polarizability makes Rydberg atom very sensitive to an external electric field. Therefore Rydberg atom becomes an ideal candidate and widely used for precise measurements of the electric fields [2–7] and microwave field [8, 9] in recent years. In other hands, Rydberg level can be tuned to the Förster resonance by applying a weak electric field, resulting in strong dipole interaction and dipole blockade effects [10–13]. The blockade effect of Rydberg atoms is employed to study the quantum logic gates [14, 15], quantum information [16], single-photon sources [17–19] and transistors [20, 21] and so on. The alkali-metal atoms are monovalent systems that allow for very accurate comparison between experiment and theory. Thus the accurate measurements of atomic polarizabilities of alkali-metal atoms are of particular interest.

The investigation of interaction between atoms and electric field can date back to 1912, when Stark observed the splitting and shifts of atomic spectral lines under the electric field, called Stark effect. Later, the Stark effect has been investigated theoretically and experimentally with different samples, such as alkali-metal as rubidium and cesium atoms and alkaline-earth metal as cadmium and mercury atoms [22]. Lots of groups have measured and calculated polarizabilities of alkali-metal atoms [23–37], such as sodium [25], rubidium [26–29] and cesium [30–37]. The Stark shifts of $n(10$–$13)S_{1/2}$ cesium states and related polarizabilities have been measured using two atomic beams [31]. Measurements of polarizabilities and hyperfine constants of cesium $(7$–$10)D_{3/2,5/2}$ states have been presented [34, 35] via the fluorescence spectroscopy of the $nD_{3/2} \rightarrow 6P_{1/2}$ transition. The Stark map and corresponding polarizabilities of cesium $(39$–$50)D_{3/2,5/2}$ Rydberg states were obtained in a conventional magneto-optical trap (MOT) by the

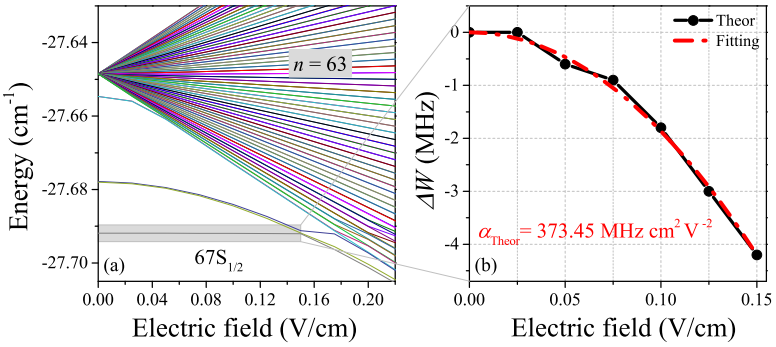

Figure 1. (a) Stark map in the vicinity of $67S_{1/2}$ Rydberg state and $n = 63$ manifolds with $|m_j| = 1/2$. Unmarked states below the manifolds are the G and F states. (b) Stark shift of $67S_{1/2}$ Rydberg state that shows an enlargement of the gray square in (a). The fitting (red dot-dash line) of the equation (3) to calculated Stark shifts (black symbols) yields a polarizaility of $67S_{1/2}$ of $\alpha_{\rm Theor} = 373.45\,{\rm MHz\,cm^2\,V^{-2}}$. The energy of $67S_{1/2}$ without electric field is set as the relative zero energy.

state-selective field ionization technique [36]. The static electric-dipole scalar and tensor polarizabilities of Rb and Cs for the $50(S, P_{1/2,3/2}, D_{3/2,5/2})$ states have been calculated within a method of an effective one-electron approximation [38].

In this work, we investigate high resolution Stark spectra of nS Rydberg states within a cold gas for higher principal quantum numbers of $n = 65$–75, which allows us to precisely measure polarizabilities of atoms. The Stark shifts of Rydberg state are attained by analysing Stark spectra. We present the precise measurements of polarizabilities of cesium nS Rydberg states. The theoretical simulations of the Stark map are reproduce the experiments well, calculated the polarizabilities are consist with the measurements. The n dependence of polarizability is also investigated and follows the $A \cdot (n^*)^7 + B \cdot (n^*)^6$ (n^* is effective principal quantum number) scaling law.

2. Theoretical model

To calculate the Stark map of cesium nS Rydberg states, we refer to the method of reference [39] and briefly describe the model here. The Hamiltonian of an atom under the external electric field is written as,

$$H = H_0 + H_{\rm I}, \tag{1}$$

with H_0 the field-free Hamiltonian and $H_{\rm I}$ the interaction Hamiltonian between atom and electric field. Considering Rydberg electron being far from the nucleus, its potential energy, $V(r)$, can be approximated as Coulomb potential. The external electric field is set along z-axis, $H_{\rm I}$ is simply written as $H_{\rm I} = Ez$ with E the value of electric field. Then Schrödinger equation is given as,

$$H\Psi = (H_0 + H_{\rm I})\Psi = (-\frac{1}{2}\nabla^2 - \frac{1}{r} + Ez)\Psi = \varepsilon\Psi. \tag{2}$$

In order to obtain the solutions of the Schrödinger equation of equation (2), we set $x = \ln r$ and $X = R\sqrt{r}$ and rewrite the radial equation, R, to the form of Numerov as $\mathrm{d}^2X/\mathrm{d}x^2 = g(x)X$. We numerical resolve the radial equation based on the method of reference [39] and attain the eigenvalues of the matrix equation under different electric-field values, further Stark map of the atoms. In figure 1(a), we present the calculation of the Stark map in the vicinity of $67S_{1/2}$ Rydberg state and $n = 63$ manifolds with $|m_j| = 1/2$. The high-l ($l > 4$) manifolds clearly show linear Stark shifts, whereas low-l states display nonlinear Stark shift. The $nS_{1/2}$ state is located below the $(n-4)$ manifolds due to the quantum defect and shows strong mixing and avoided crossings with high-l manifolds states as nS state has smaller fraction quantum defect [40]. For investigating the Stark shift of $nS_{1/2}$ Rydberg state, we enlarge the gray square marked area of figure 1(a). It is clearly seen the nonlinear Stark shift depending on the external electric field.

The energy shift of atoms due to the external field, ΔW, depends on its polarizability, α, expressed as [22],

$$\Delta W = -\frac{1}{2}\alpha E^2 = -\frac{E^2}{2}[\alpha_0 + \alpha_2 \frac{3\,\mathrm{m}_j^2 - j(j+1)}{j(2j-1)}], \tag{3}$$

with α_0 (α_2) scalar (tensor) polarizability and j (m_j) angular (magnetic) quantum number. For cesium S-type ($l = 0$) atoms, $j = |m_j| = 1/2$, $\alpha_2 = 0$. The polarizability of nS Rydberg atom $\alpha = \alpha_0$, corresponding Stark map only display energy shift. Nevertheless, there is still a tiny tensor polarizability when considering

Table 1. Comparison of measurements and calculations of polarizabilities (in MHz cm^2 V^{-2}) of $nS_{1/2}$ Rydberg states, error bars display the fitting errors of equation (3). κ displays relative deviation defined as $\kappa = (|\alpha_{\rm Exp} - \alpha_{\rm Theor}|)/\alpha_{\rm Theor}$.

n	$\alpha_{\rm Theor}$	$\alpha_{\rm Exp}$	κ
65	307.13 ± 6.24	301.25 ± 6.01	0.019
67	373.45 ± 7.00	373.72 ± 7.68	0.001
70	460.18 ± 14.48	457.57 ± 6.13	0.006
73	678.93 ± 13.29	667.76 ± 5.74	0.016
75	729.14 ± 15.30	727.32 ± 3.97	0.003

the hyperfine structure, which we ignore here [22]. For ($l \geqslant 1$) state, atom possess non-zero tensor polarizability, corresponding Stark map displays both energy shift and splitting. For the $67S_{1/2}$ state of figure 1(b), the fitting of the equation (3) yields the polarizability of $67S_{1/2}$ state, $\alpha = 373.45$ MHz cm^2 V^{-2}, see red dot-dashed line of figure 1(b). We attain the polarizabilities for large quantum number n using the same method, displayed in table 1.

3. Experiment and analysis

3.1. Experimental method

The experiment is performed in a standard cesium MOT with the chamber vacuum 2×10^{-7} Pa. The MOT sample has a temperature $\sim$100 μK and peak density $\sim 10^{10}$ cm^{-3}, measured by an absorption imaging. Figure 2 displays the schematic diagram of the experiments. Two-photon scheme, see figure 2 inset, is employed to achieve the Rydberg excitation. An 852 nm (Toptical DLpro), and a 510 nm (Toptical DLpro + Precilasers YFL-SHG-509-1.5) lasers, are overlapped in a counter propagating geometry through the MOT center. The frequency of 852 nm laser is locked on the resonance transition, $|6S_{1/2}, F = 4\rangle \rightarrow |6P_{3/2}, F' = 5\rangle$, with a polarization spectroscopy (PS) [41], which frequency is 360 MHz blue-detuned from the intermediate $|6P_{3/2}\rangle$ state by a double-pass acousto-optic modulator (AOM). The 510 nm laser is produced by frequency doubling of a 1020 nm laser whose frequency is stabilized to an ultra-stable Fabry–Perot (F–P) cavity with a finesse of 15 000 employing Pound–Drever–Hall (PDH) method. The frequency then is tuned to the Rydberg resonance transition by varying the radio-frequency signal (RF) applied to the electro-optic modulator (EOM) that is used to lock the laser to the F–P cavity.

The waist of the 852 nm (510 nm) beam at MOT center is 80 (40) μm, forming the cigar-shaped excitation volume. In order to avoid the effect of interaction between Rydberg atoms on the polarizabilities measurements, we use small 852 nm (510 nm) power 0.02 (4.7) mW, corresponding energy shift due to interaction to be less than 100 kHz, which yields a negligible effect on the polarizabilities measurements of this work.

In addition, three pairs of electrodes are placed beside the excitation region in three directions, not shown in figure 2, where we apply external electric fields for ionizing the Rydberg atom and compensating the stray electric field. During the experiment, after switching off MOT beams, we turn on the Rydberg excitation pulse (1 μs) and then a ramped ionization electric field (ramp time 3 μs) to ionize the Rydberg atoms. The resultant Rydberg ions are collected with a MCP detector with a 10% collection efficiency and sampled with a boxcar (SRS-250) and recorded with a computer. To attain accurately an electric field value atoms experienced, (i) we calibrate the electric field produced by applying a potential at electrodes with the Maxwell program. The simulation shows that the electric field value at MOT center is 36% of z-direction and 68% of y-direction less than the calculated electric value of U/d with U the applied potential and d the distance between two electrode plates. (ii) We compensate the stray electric field at the MOT center by the Stark map of $70D_{5/2}$, measured Stark map of z-direction is shown in figure 3, from which compensation electric field is 0.046 V cm^{-1}. We do similar measurements as figure 3 in x- and y-directions, corresponding field around MOT is expected to be less than 30 mV cm^{-1} after compensating the stray field of three directions.

3.2. Results and analysis

Figure 4(a) presents measurements of Stark shifts as a function of applied electric fields. In the inset of figure 4(a), we displays a typical spectrum of $75S_{1/2}$ Rydberg state at electric field 0.04 V cm^{-1}. The spectrum of Rydberg state is obtained by scanning the RF that is applied to the EOM used to lock the second excitation (510 nm) laser to the F–P cavity. Gaussian fitting (blue line of figure 4(a) inset) to the spectrum yields a peak center, corresponding Stark shift of -0.71 MHz, and linewidth of Rydberg excitation

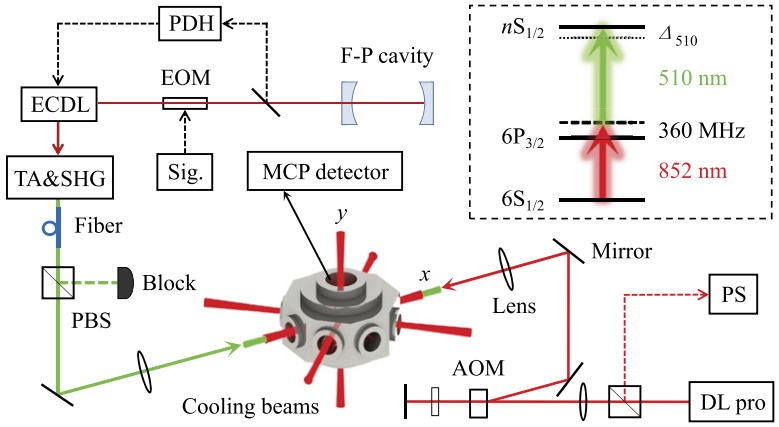

Figure 2. Experimental schematic of two-photon Rydberg excitation. The frequency of 852 nm is stabilized to the lower transition by a PS method and 360 MHz blue-detuned of the intermediate level with a double-pass AOM. The frequency of 510 nm laser comes from the frequency double (TA & SHG) of 1020 nm ECDL laser whose frequency is locked to an F–P cavity with the PDH method. The EOM is used to tune the 510 nm frequency to achieve Rydberg excitation. Two lasers counter propagate along the x direction and overlapped at the MOT center. Rydberg atoms are ionized with ramped electric field and detected with a microchannel plate (MCP) detector. Inset displays the two-photon excitation diagram. The first photon (852 nm) drives the lower transition $|6S_{1/2}\rangle \rightarrow |6P_{3/2}\rangle$, whereas the second photon (510 nm) drives the Rydberg transition $|6P_{3/2}\rangle \rightarrow |nS_{1/2}\rangle$.

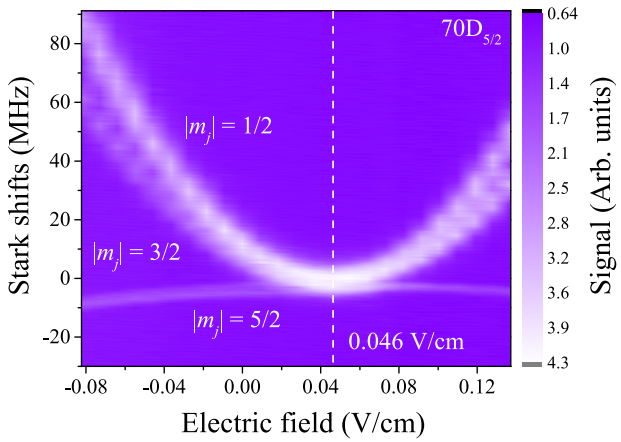

Figure 3. Color map of Stark spectra of $70D_{5/2}$ in the z-direction. The spectroscopy shows symmetrical Stark splitting, corresponding to $|m_j| = 1/2, 3/2, 5/2$. The zero field represents the potential applied to the electrode $U = 0$. Vertical white dashed line indicates compensation electric field of 46 mV cm^{-1} in z direction, where there is no Stark shifts and splitting, corresponding zero field atoms experienced.

of 2.72 MHz. We do a series of measurements of Rydberg spectra under electric fields and attain the Stark map of figure 4(b). It is noted that the field values used here are set to be smaller than the field value the first avoiding cross appears in the Stark map. As mentioned above, for nS state with $l = 0$ and the magnetic quantum number $|m_j| = 1/2$, the Stark map only shows negative Stark shifts without splitting. We fit measurements of figure 4(a) with equation (3) and attain polarizabilitiy $\alpha_{\rm Exp} = 727.32 \pm 3.97$ MHz cm^2 V^{-2}. For comparison, in figure 4(a), we also display calculations of Stark shifts and related polarizability $\alpha_{\rm Theor} = 729.14 \pm 15.30$ MHz cm^2 V^{-2}, showing a good agreements between calculation and measurement.

Close inspection of Stark map in figure 4(b) reveals that the linewidth of the Rydberg spectra is nearly kept same when the electric field varies. The spectroscopy displays the perfect symmetry of atomic Stark shifts when we apply reverse potential on the electrode plates.

We do a series of measurements like figure 4 for the range of $n = 65$–75, measured polarizabilities are displayed in table 1, together with the calculations. We introduce the relative deviation by formula $\kappa = (|\alpha_{\rm Exp} - \alpha_{\rm Theor}|)/\alpha_{\rm Theor}$ to indicate an accuracy of our experiments, corresponding κ is displayed in fourth column of the table 1. For $75S_{1/2}$ of figure 4, the relative deviation $\kappa = 0.3\%$. It is found that the measurements show consistent with theoretical calculations with relative deviations less than 2%. For the experiments, the error mainly comes from a few sources. The first is the accuracy of the frequency of the Rydberg excitation lasers, both 852 nm and 510 nm lasers are calibrated with the wavelength meter

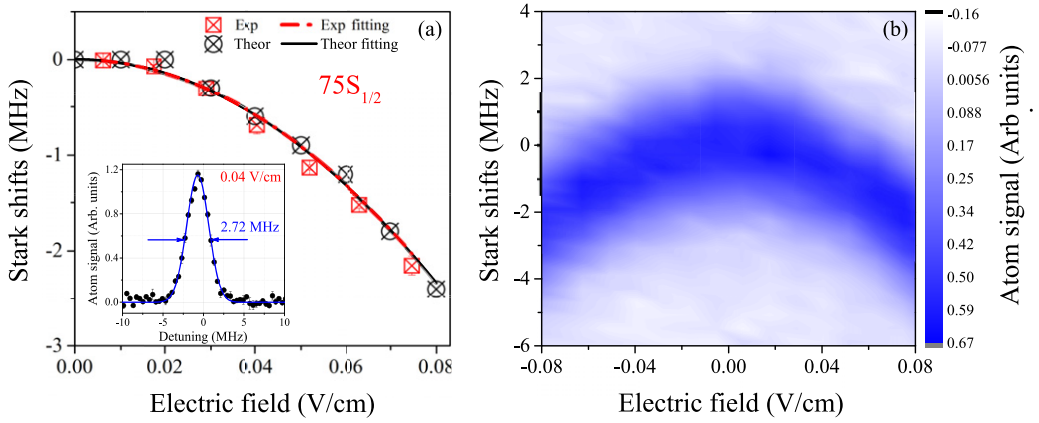

Figure 4. (a) Measurements (red squares) and calculations (black circles) of the Stark shifts of $75S_{1/2}$ Rydberg atoms. The fittings to the data with equation (3) yield a polarizabilitiy of $\alpha_{\rm Exp} = 727.32 \pm 3.97$ MHz cm^2 V^{-2} and $\alpha_{\rm Theor} = 729.14 \pm 15.30$ MHz cm^2 V^{-2}, respectively. Error bars of data display the standard error of two independent measurements. Inset presents a typical spectrum of $75S_{1/2}$ Rydberg state with high resolution under an electric field 0.04 V cm^{-1}, solid line displays Gaussian fitting to the spectrum, related peak center -0.71 MHz and spectral linewidth 2.72 MHz. (b) Intensity distribution diagram of Stark map with calibrated electric field values.

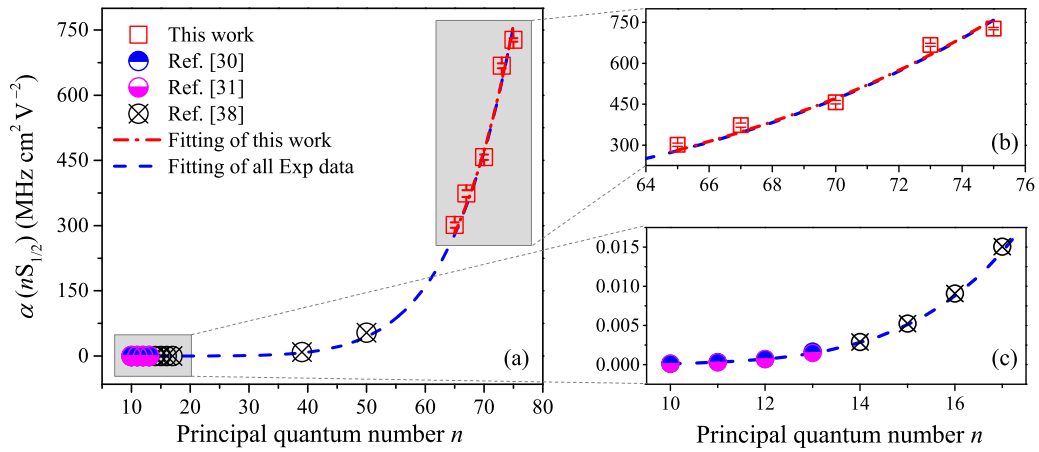

Figure 5. (a) Polarizabilities of nS states as a function of principal quantum number shown with red squares for this work, blue semicircles [30], pink semicircles [31] and black circles of calculation [38], respectively. The n^* dependence of polarizabilities is obtained by fitting of equation (4) to the data of this work (red dot-dashed line) and all data (blue dashed line). The fitting lines to this work $n = 65$–75 and to all data $n = 10$–75 demonstrate overlap well each other. Coefficients $A = 5.62 \times 10^{-11}$ and $B = 2.52 \times 10^{-9}$. (b) and (c) are enlargements of the gray square marked parts of $65 \leqslant n \leqslant 75$ and $10 \leqslant n \leqslant 17$ in (a), respectively.

(HF-Angstrom WSU-30) and the second excitation 510 nm laser is locked to the F–P cavity with finesse of 15 000, corresponding laser linewidth less than 50 kHz. The second is fitting error including the Gaussian fitting to the atomic spectrum for obtaining the Stark shift and fittings of equation (3) for attaining the polarizabilities. The deviation due to Gaussian fitting of the Rydberg field ionization spectroscopy is $\lesssim 40$ kHz. The third is the electric field value the Rydberg atom experienced, that is calibrated with Stark map of $70D_{5/2}$, see figure 3. The estimated stray electric field is less than 30 mV cm^{-1} after compensating, leading to the Rydberg level-shift range between 100 kHz at $n = 65$ and 300 kHz at $n = 75$. Finally is the energy shifts due to the long-range interaction between Rydberg atoms. For n range and Rydberg density of $\sim 2 \times 10^8$ cm^{-3} used in this work, estimated long-range interaction (C_6/R^6 with C_6 dispersion parameter) between Rydberg atoms is less than 100 kHz, yielding a negligible effect for Rydberg level shifts. This is corroborated by measured Stark spectrum showing nice Gaussian profile, see figure 4(a) inset.

It is seen that, from the table 1, the polarizability demonstrates a fast increasing with the principal quantum number. For instance, the polarizability, 301.25 ± 6.01 MHz cm^2 V^{-2} for $65S_{1/2}$ is increased to 727.32 ± 3.97 MHz cm^2 V^{-2} for $75S_{1/2}$ state. The dependence of polarizability of Rydberg atom on effective quantum number $n^* = (n - \delta)$ is expressed as [26, 27]

$$\alpha = A \cdot (n^*)^a + B \cdot (n^*)^b, \tag{4}$$

Table 2. Fitting parameters a and b in figure 5. * indicates the fitting with the coefficient $A = 6.62 \times 10^{-11}$ from [37].

	a	b
Fitting of all exp. data	6.98 ± 0.02	5.98 ± 0.01
Fitting of all exp. data*	6.95 ± 0.01	5.97 ± 0.01
Fitting of this work	6.96 ± 0.29	6.00 ± 0.39

with A and B the coefficients, ($A = 5.62 \times 10^{-11}$ and $B = 2.52 \times 10^{-9}$) [27, 37], and $\delta = 4.05$ the quantum defect of $nS_{1/2}$ state [42]. In order to attain the scaling law of polarizability, in figure 5(a) we plot measurements of polarizabilities versus principal quantum number n and fitting of equation (4) to the data of $n = 65$–75 (red dot-dashed line). The fitting parameter is $a(b) = 6.96 \pm 0.29$ (6.00 ± 0.39).

For further comparison with the previous work, we also display measurements for $n = 10$–13 [30, 31] and calculations for $n = 14$–$17, 39, 50$ [38] of polarizabilities in figure 5(a). It is seen that the polarizability of lower n is much smaller than that of the higher n of this work. We fit polarizabilities of $n = 10$–75 including previous measurements of low n using equation (4), see a blue dashed line of figure 5(a), corresponding fitting parameter $a(b) = 6.98 \pm 0.02$ (5.98 ± 0.01). In table 2, we display fitting parameters for comparison, the deviation between the fitting parameters for two n-range is 0.2% (0.3%) for a (b). To demonstrate the details, we enlarge gray regions of figure 5(a) in figure 5(b) for high n and figure 5(c) for lower n. It is found that both fitting lines overlap each other, which means that the n^* scaling $A \cdot (n^*)^7 + B \cdot (n^*)^6$, the expression extracted with $n = 15$–55 [37], can be extended to higher n, for example $n = 75$ of this work, but with slightly modification of the coefficient A. In the table 2, we also present fitting results for $A = 6.62 \times 10^{-11}$ of reference [37] for comparison.

4. Conclusion

We have obtained high resolution Stark spectra of $nS_{1/2}$ ($n = 65$–75) Rydberg states under external electric fields. The polarizabilities of cesium $nS_{1/2}$ Rydberg states are attained experimentally and theoretically by analyzing Stark shifts, showing an agreement well between measurements and calculations. The scaling of principal quantum number n has been attained employing equation (4) to fit the data of this work $n = 65$–75 and data including previous works, and both fitting lines show agreement well with each other. The n^* scaling $A \cdot (n^*)^7 + B \cdot (n^*)^6$, the expression extracted with $n = 15$–55, can be extended to higher n, $n = 75$ of this work. Polarizability is an intrinsic property of an atom, which plays a key role in atomic physics. Precise measurements of polarizabilities of Rydberg atoms are of significance not only for fundamental physics but also for practical applications of modern quantum technologies using such Rydberg atoms, for instance the Rydberg atom based measurements of weak electric fields and microwave fields.

Acknowledgments

The work is supported by the National Key R & D Program of China (Grant No. 2017YFA0304203), the National Natural Science Foundation of China (Grant No. 11434007, 61835007, 61675123, 61775124 and 11804202), and Changjiang Scholars and Innovative Research Team in University of Ministry of Education of China (Grant No. IRT_17R70) and 1331 Project of Shanxi Province.

ORCID iDs

Jianming Zhao https://orcid.org/0000-0001-8420-9319

References

[1] Gallagher T F 1994 *Rydberg Atoms* (Cambridge: Cambridge University Press)
[2] Jiao Y, Han X, Yang Z, Li J, Raithel G, Zhao J and Jia S 2016 *Phys. Rev.* A **94** 023832
[3] Jiao Y, Hao L, Han X, Bai S, Raithel G, Zhao J and Jia S 2017 *Phys. Rev. Appl.* **8** 014028
[4] Jing M, Hu Y, Ma J, Zhang H, Zhang L, Xiao L and Jia S 2020 *Nat. Phys.* (https://doi.org/10.1038/S41567-020-0918-5)
[5] Holloway C L, Gordon J A, Jefferts S, Schwarzkopf A, Anderson D A, Miller S A, Thaicharoen N and Raithel G 2014 *IEEE Trans. Antennas Propag.* **62** 6169
[6] Holloway C L, Simons M T, Gordon J A, Dienstfrey A, Anderson D A and Raithel G 2017 *J. Appl. phys.* **121** 233106
[7] Hao L, Xue Y, Fan J, Bai J, Jiao Y and Zhao J 2020 *Chin. Phys.* B **29** 033201

[8] Sedlacek J A, Schwettmann A, Kübler H, Löw R, Pfau T and Shaffer J P 2012 *Nat. Phys.* **8** 819
[9] Bai J, Fan J, Hao L, Spong N L R, Jiao Y and Zhao J 2019 *Appl. Sci.* **9** 4895
[10] Vogt T, Viteau M, Zhao J, Chotia A, Comparat D and Pillet P 2006 *Phys. Rev. Lett.* **97** 083003
[11] Comparat D and Pillet P 2010 *J. Opt. Soc. Am.* B **6** A208
[12] Ates C, Pohl T, Pattard T and Rost J M 2006 *J. Phys. B: At., Mol. Opt. Phys.* **39** L233
[13] Reinhard A, Liebisch T C, Knuffman B and Raithel G 2007 *Phys. Rev.* A **75** 032712
[14] Isenhower L, Urban E, Zhang X L, Gill A T, Henage T, Johnson T A, Walker T G and Saffman M 2010 *Phys. Rev. Lett.* **104** 010503
[15] Urban E, Johnson T A, Henage T, Isenhower L, Yavuz D D, Walker T G and Saffman M 2009 *Nat. Phys.* **5** 110
[16] Lukin M D, Fleischhauer M, Cote R, Duan L M, Jaksch D, Cirac J I and Zoller P 2001 *Phys. Rev. Lett.* **87** 037901
[17] Saffman M and Walker T G 2002 *Phys. Rev.* A **66** 065403
[18] Dudin Y O and Kuzmich A 2012 *Science* **336** 887
[19] Peyronel T, Firstenberg O, Liang Q Y, Hofferberth S, Gorshkov A V, Pohl T, Lukin M D and Vuletić V 2012 *Nature* **488** 57
[20] Gorniaczyk H, Tresp C, Schmidt J, Fedder H and Hofferberth S 2014 *Phys. Rev. Lett.* **113** 053601
[21] Tiarks D, Baur S, Schneider K, Dürr S and Rempe G 2014 *Phys. Rev. Lett.* **113** 053602
[22] Khadjavi A, Lurio A and Happer W 1968 *Phys. Rev.* **167** 128
[23] Molof R W, Schwartz H L, Miller T M and Bederson B 1974 *Phys. Rev.* A **10** 1131
[24] Hall W D and Zorn J C 1974 *Phys. Rev.* A **10** 1141
[25] Ekstrom C R, Schmiedmayer J, Chapman M S, Hammond T D and Pritchard D E 1995 *Phys. Rev.* A **51** 3883
[26] O'Sullivan M S and Stoicheff B P 1986 *Phys. Rev.* A **33** 1640
[27] O'Sullivan M S and Stoicheff B P 1985 *Phys. Rev.* A **31** 2718
[28] Safronova M S and Safronova U I 2011 *Phys. Rev.* A **83** 052508
[29] Walls J, Clarke J, Cauchi S, Karkas G, Chen H and van Wijngaarden W A 2001 *Eur. Phys. J.* D **14** 9
[30] Fredriksson K and Svanberg S 1977 *Z. Phys.* A **281** 189
[31] van Wijngaarden W A, Hessels E A, Li J and Rothery N E 1994 *Phys. Rev.* A **49** R2220
[32] Tanner C E and Wieman C 1988 *Phys. Rev.* A **38** 162
[33] Amini J M and Gould H 2003 *Phys. Rev. Lett.* **91** 153001
[34] Auzinsh M, Blushs K, Ferber R, Gahbauer F, Jarmola A and Tamanis M 2006 *Opt. Commun.* **264** 333
[35] Auzinsh M, Bluss K, Ferber R, Gahbauer F, Jarmola A, Safronova M S, Safronova U I and Tamanis M 2007 *Phys. Rev.* A **75** 022502
[36] Zhao J, Zhang H, Feng Z, Zhu X, Zhang L, Li C and Jia S 2011 *J. Phys. Soc. Jpn.* **80** 034303
[37] He X, Li B and Zhang C 1989 *Acta Phys. Sin.* **38** 1717 [in Chinese]
[38] Yerokhin V A, Buhmann S Y, Fritzsche S and Surzhykov A 2016 *Phys. Rev.* A **94** 032503
[39] Zimmerman M L, Littman M G, Kash M M and Kleppner D 1979 *Phys. Rev.* A **20** 2251
[40] Zhang H, Wang L, Zhang L, Li C, Xiao L, Zhao J and Jia S 2013 *Phys. Rev.* A **87** 033405
[41] Pearman C P, Adams C S, Cox S G, Griffin P F, Smith D A and Hughes I G 2002 *J. Phys. B: At. Mol. Opt. Phys.* **35** 5141
[42] Deiglmayr J, Herburger H, Saßmannshausen H, Jansen P, Schmutz H and Merkt F 2016 *Phys. Rev.* A **93** 013424